Journal of Electrostatics

EVALUATING THE ELECTROSTATIC DISCHARGE RISK BETWEEN SMALL RADIUS OBJECTS AND CHARGED PLANAR INSULATING MATERIALS

--Manuscript Draft--

Manuscript Number:	ELSTAT-D-21-00206R1
Article Type:	SI: Electrostatics 2022
Section/Category:	
Keywords:	Modeling; Electric field; Charge transfer; Electrostatic field measurements; electrostatic discharge risk evaluation
Corresponding Author:	Jeremy Smallwood, PhD Electrostatic Solutions Ltd Southampton, UNITED KINGDOM
First Author:	Jeremy Smallwood
Order of Authors:	Jeremy Smallwood
	Nicolas G. Green, PhD
	Kelly Robinson
Manuscript Region of Origin:	Europe
Abstract:	In some industrial situations such as web processes, charging of large planar insulating surfaces can give risk of electrostatic discharges that could ignite flammable process materials such as solvent vapours. Charging of the material has for some years been evaluated using electrostatic field measurements to estimate surface charge densities. In a planar system, the threshold risk of an electrostatic discharge has been equated with a surface charge density of about 25 μCm-2 required to produce a field strength exceeding about 3 MVm-1, the breakdown field strength of air. It is known that where a small radius earthed conducting object approaches a charged insulator, intensification of the field strength occurs at the surface of the object. Similarly, the field strength is increased by the presence of a field meter near the surface. This paper investigates the effect of field concentration by an object near the charged insulator and the conditions leading to electrostatic discharges using analysis, electrostatic field modelling and experiments. The results are applied to understanding and quantification of the effect on measurements and safety factor indicated for evaluation of electrostatic discharge risk introduced by the earthed conductor in this situation.
Response to Reviewers:	

Reviewer comment	Author's responses
Reviewer #1: This manuscript presents some interesting quantitative studies on the electrostatic processes between an insulating plane and a spherical electrode. However, in order to be accepted for journal publication, the manuscript needs major revision and significant improvements. In addition, the quality of several figures is low; there are some typos which should have been corrected during proofreading; the citation of most references also needs to follow journal's guideline.	Thank you for your interesting and useful comments and questions. We have made revisions and improved figures.
1. The entire Section 5 is missing.	Sec. 5 has been inserted.
2. In Section 3, the equations underlying the curves in Figs. 4-7 should be provided.	Equations added for each Figure Figure 6 has been deleted and following figures renumbered.
3. Figure 2 the experimental setup. "18 mm" in the 4th line above the figure should be "18 cm"? Later the authors mentioned field linearization plates, which are not presented in this figure.	18 mm is the correct figure covering when the PTFE target is horizontal above the ground plane. We have added a few words to clarify.
4. Figure 4 y-axis. The unit of electric field should be kV/mm, not V/mm.	Units of electric field in Figure 4 corrected. Thank-you.
5. Figure 7 needs some clarification. It seems that for distance 0 the charge density has some value. How is it possible?	Discussion is added describing why the charge density increases for gaps D less than 1 cm. Added also is a note that the focus of this work is on discharges that occur at larger gaps when the charge density exceed the minimum value.
6. Figure 9 (new Figure 8): it would be much more informative to include the spread of the measurement results.	We certainly appreciate that variability in measured results is important. This figure, however, illustrates the results of computer modelling in which there is no experimental variation in results.
7. Figure 12 seems redundant. All information has been included in Figure 11.	Fig 12 has been deleted
8. Figure 14: why in some cases the transferred charge is zero?	Where the charged transferred is zero presumably no discharge has taken place. We have added discussion to the text
9. Figure 15 and Figure 16: how did the authors determine the time and position of the movement by hand?	The electrode was mounted on a retort stand held in position against a guide fitted with a rule. This maintained the probe on the axis of the target as the distance was varied by hand. A pointer on the retort stand indicated the electrode-target gap. (± 1 mm). After setting the recorder running the retort stand was moved by hand towards the target. The speed of approach was not accurately controlled but was reasonably representative of a speed that might be used in practical ignition tests (in which the probes are typically hand held and manipulated. We have added clarification of the arrangement in Section 2 and improved the description in 6.4.
10. Table 1: why are some data missing?	We have reviewed the table and deleted two of the rows concerned. The remaining row was an example

	of a “no discharge” result and the gaps have been filled accordingly

Reviewer comment	Author’s responses
Reviewer #2: The paper deals with a very interesting and a very important practical problem of the risk assessment of the electrostatic discharge. This discharge can lead to explosions, whose probability needs to be reduced. The paper presents a new model for evaluating the effect of electric field concentration for the situation when a small conducting object approaches a charged insulating surface. The paper is original and it contributes to a better understanding of the process. In my opinion, it fully deserves to be published after some issues listed below have been addressed.	Thank you for your interesting and useful comments and questions.
1. Section 2, first paragraph below Fig.1: "the PTFE target was charged with corona discharge to create a reasonably constant surface charge density" - what does it mean "reasonable"? Was the charge uniformity verified?	This is a good point. The local charge density variation was not verified and variation across the surface and between experiments can be expected. Nevertheless the experiments depends more on the total effect of charge on the region around the target axis rather than small area local charge density (except perhaps for breakdown across small gaps) . Our field measurements and induced charge on the electrode (e.g. Figure 9) confirmed reasonably reproducible results. Some discussion has been added in 6.1.
2. Section 2, second paragraph below Fig.1: "approximately 18 mm above a ground plane". I would think this distance has a strong effect on the deposited surface charge density. Why was this not fixed to a precise value? Why was the insulating surface not lying on the ground plane?	The minimum distance was dictated by the construction of the apparatus frame from tubular polymer material. Some variation was caused by warping of the PTFE sheet, for example under gravity and due to imperfections in the frame construction. We considered it advantageous to have the target a distance from the underlying ground plane during charging as this reduced the strength of charging and gave improved charging uniformity, reducing the effect of gap variations which were difficult to avoid. We have added some explanation under Fig 1.
Page 3, Fig.2: This Figure doesn't really provide any new information to that in Fig.1. The same with Fig. 3 on page 4.	We have replaced Fig 2 with a photograph showing instead the EFM51 field meter mounted in the place of the electrodes and details such as the ground plane and guide with rule, and the EFM51 with field plate
Page 4, Fig. 4: is this Figure copied from literature. If yes, please provide a reference.	This is an original figure from one of the authors based on the theoretical considerations given.
Page 7, Fig.8: this diagram suggests that the surface charge density was present on both sides of the charged insulating sheet. Is this true? This may be	The surface charge density was on one side of the target only.

quite different than in the case of a one side charging.	
Page 12, Table 1: How to interpret the empty cells in this Table?	We have reviewed the table and deleted two of the rows concerned. The remaining row was an example of a “no discharge” result and the gaps have been filled accordingly
Page 12, Section 7.1: I don't quite understand this discussion. It is obvious that the presence of the linearizing plate changes the electric field distribution. Why "in normal use with gap around 25 mm the field would be overestimated approximately by a factor of 2"?	We don’t understand the difficulty here. The field meter used as supplied, at a distance of 25 mm, without a plate gives twice the reading than when fitted with a plate. Our results are consistent with the meter reading being correct when fitted with the plate. We have rewritten the paragraph in an attempt to make it clearer.
8. Page 14, References: I have spotted numerous typos. Moreover, I don't really understand why some parts are highlighted.	Our apologies. We were aware the references needed clarification and checking and the highlighting was to help us with this. We hope you now find the references acceptable.

EVALUATING THE ELECTROSTATIC DISCHARGE RISK BETWEEN SMALL RADIUS OBJECTS AND CHARGED PLANAR INSULATING MATERIALS

Jeremy Smallwood[1], Nicolas G. Green[2], Kelly Robinson[3]

Highlights

- Electrostatic field concentration by an earthed conductor near a charged insulator
- Comparison using analytical, computer modelling and experimental techniques.
- Electrostatic discharges investigated for electrodes used in ignition hazard evaluation
- Onset of discharges depended on electrode surface charge density and diameter
- Smaller electrode gave discharges at lower induced charge threshold
-

EVALUATING THE ELECTROSTATIC DISCHARGE RISK BETWEEN SMALL RADIUS OBJECTS AND CHARGED PLANAR INSULATING MATERIALS

Jeremy Smallwood[1], Nicolas G. Green[2], Kelly Robinson[3]

[1] *Electrostatic Solutions Ltd, 13 Redhill Crescent, Southampton, SO16 7BQ, UK.*
tel.: +44 23 8090 5600, e-mail: jeremys@static-sol.com

[2] *University of Southampton, Highfield, Southampton, UK*

[3] *Electrostatic Answers LLC, 15 Piping Rock Run, Fairport NY 14450-9596, USA*

Abstract

In some industrial situations such as web processes, charging of large planar insulating surfaces can give risk of electrostatic discharges that could ignite flammable process materials such as solvent vapours. Charging of the material has for some years been evaluated using electrostatic field measurements to estimate surface charge densities. In a planar system, the threshold risk of an electrostatic discharge has been equated with a surface charge density of about 25 μCm^{-2} required to produce a field strength exceeding about 3 MVm-1, the breakdown field strength of air. It is known that where a small radius earthed conducting object approaches a charged insulator, intensification of the field strength occurs at the surface of the object. Similarly, the field strength is increased by the presence of a field meter near the surface. This paper investigates the effect of field concentration by an object near the charged insulator and the conditions leading to electrostatic discharges using analysis, electrostatic field modelling and experiments. The results are applied to understanding and quantification of the effect on measurements and safety factor indicated for evaluation of electrostatic discharge risk introduced by the earthed conductor in this situation.

Initiation of a discharge to a spherical measurement electrode requires that the field strength at the surface of the electrode exceeds the breakdown field strength and other factors. This occurs at different induced charge levels on the electrode for different electrode diameter. Discharges could occur with electrode-target gap around 10-20 mm at lower charge density than with smaller gaps. The threshold of discharges occurring was reached at lower charge density for a smaller 16.6 mm diameter electrode, which might be important when evaluating ignition risk for Group IIC flammable materials. Conversely higher charge transfer was confirmed with 25.4 mm electrode above the threshold for discharges occurring.

Keywords: Modeling, Electric field, Charge transfer, Electrostatic field measurements, electrostatic discharge risk evaluation

1 Introduction

In some industrial situations such as web processes, charging of large planar insulating surfaces can give risk of electrostatic discharges that could ignite flammable process materials such as solvent vapours or gases [1], [2], [3].

Charging of the material has for some years been evaluated using electrostatic field measurements to estimate surface charge densities [4], [5]. In a planar system, the threshold risk of an electrostatic discharge has been equated with a surface charge density of about 25 $\mu C\ m^{-2}$ required to produce a field strength exceeding about 3 $MV\ m^{-1}$, the breakdown field strength of air.

The ignition risk from electrostatic discharges from charged insulators has also been evaluated by measuring the charge transferred in electrostatic discharges (ESD) drawn from the surface using spherical electrodes of various diameters [1], [3], [6], [7]. Gibson & Lloyd [1] found that the nature of the discharge changed with electrode size, changing from corona to "spark type" (probably now usually called brush discharge) as the hemispherical electrode diameter increased from 1 mm to 10 mm. The latter could ignite various flammable solvent-vapour-air mixtures.

It is known that where a small radius earthed conducting object approaches the charged insulator, intensification of the field strength occurs at the surface of the object. Similarly, the field strength is

increased by the presence of a field meter near the surface. Various workers have shown that the breakdown field strength at the surface of a spherical electrode increases with reducing electrode diameter [8], [9], [10]. The field strength at the surface of the sphere is also modified by the presence of a nearby charged conductive or insulative plane.

This paper is to use electrostatic field modelling and experiments to investigate the effect of field concentration by an object near the charged insulator. The results are applied to understanding and quantification of the effect of the earthed conductor (field meter or spherical discharge probe) in this situation on common measurements and evaluation of electrostatic discharge risk.

2 Experimental arrangement

The experimental arrangement for experimental work is shown in Figure 1, Figure 2. This is also used as the basis for analytical analysis and computer modelling.

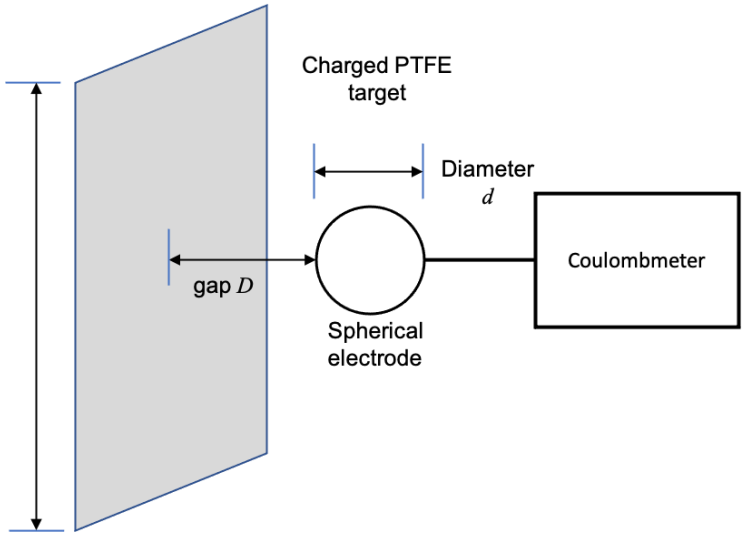

Figure 1. Experimental arrangement

In practical experiments, the PTFE target was charged with corona discharge to create a reasonably constant surface charge density. In practice the local charge density could not be verified and variation across the target surface and between experiments can be expected. This is discussed in 6.1. The charge induced on the spherical electrode at gaps *D* of 300, 250, 200, 150, 100, 50, 20, 10, and 5 mm, was measured as the electrode was brought in from a distance.

The target was charged in the horizontal position, lowered to lie approximately 18 mm above a ground plane. The charge density could be varied by variation of the corona charging voltage on 3 pins on a hand held wand that was passed in 6 passes over the entire surface, with the points approximately 10 mm from the target surface.

The target was mounted at a distance from the underlying ground plane during charging as this reduced the strength of charging and gave improved charging uniformity and reproducibility. The minimum gap between ground plane and target was dictated by the dimensions of the tubular polymer material which formed the apparatus frame. Some variation of gap was caused by warping of the PTFE sheet under gravity and due to imperfections in the frame construction. The gap had the effect of reducing the effect of gap variations which were difficult to avoid in practice.

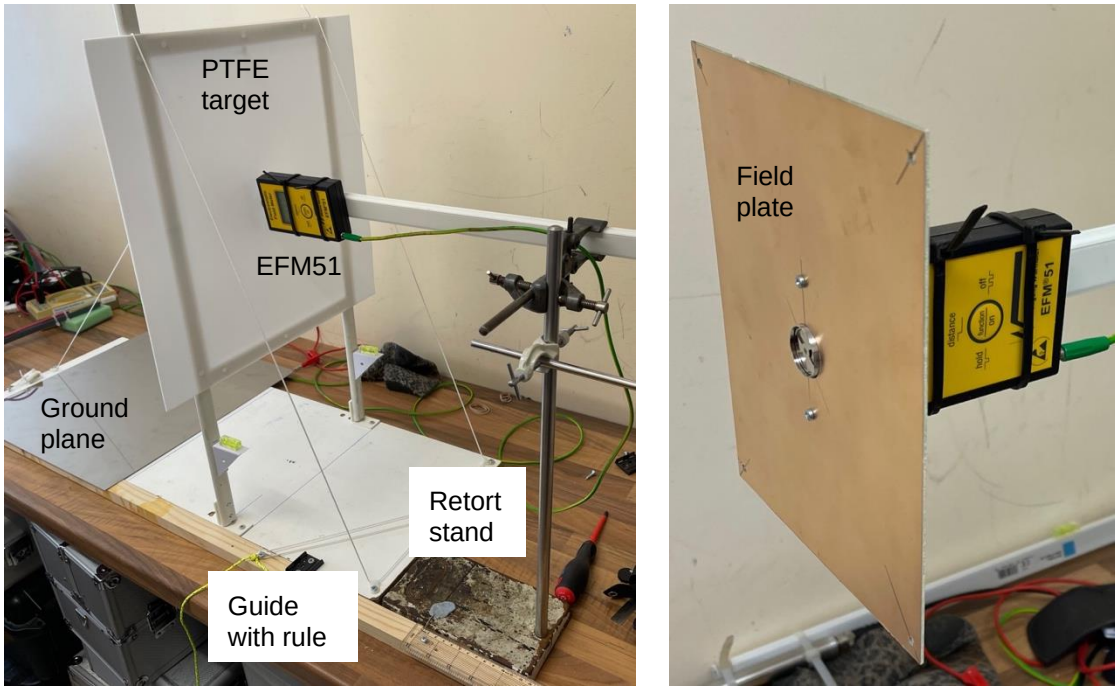

Figure 2. Practical experimental arrangement showing (left) EFM51 field meter (without field plate) fitted in apparatus in the place of electrodes and (right) field plate fitted to EFM51

The electrodes (probes) used were representative of those specified in the standards [3], [6], [7] for electrostatic discharge charge transfer measurements in electrostatic hazard evaluation. The electrode diameters were 16.6 and 25.4 mm. The spherical electrodes were mounted on an earthed metal handle that enabled handling of the probes as well as shielding the internal wiring connecting to the electrode (Figure 3). The handle terminated in a BNC connector that enabled easy connection via coaxial cable to a charge measurement system. The charge induced in the electrode or transferred in a discharge was measured using a JCI 145 coulombmeter. The probes were supported by insulating supports held in a movable metal retort stand. The stand was held against a wooden guide fitted with a rule. The guide ensured that the electrode could be moved by hand along the axis concentric with the target plane. A pointer fixed to the retort stand and moving over the rule indicated the electrode-target gap with an estimated accuracy of ± 1 mm. The electrodes could thus be set in repeatable distance positions along the axis concentric to the target and moved along the axis towards or away from the target as desired.

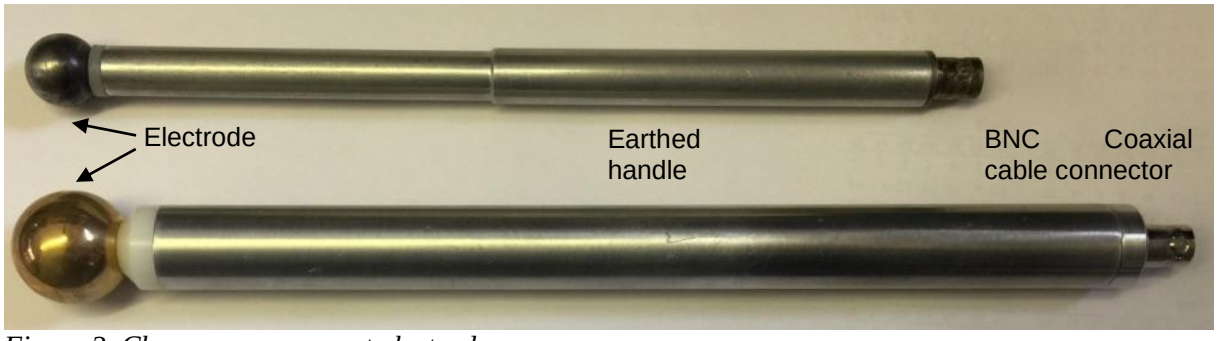

Figure 3. Charge measurement electrodes

3 Analytical work

Analytical work examined a number of aspects pertinent to an electrostatic discharge occurring between a spherical electrode and a charged planar target material. The well known Paschen's Law [11], [12] shows that the breakdown voltage and hence breakdown electrostatic field strength and charge density

is expected to vary with proximity to the charged sheet (Figure 4). The Modified Paschen's Law limits the electric field at small gaps to account for field emission and other non-linear mechanisms that were experimentally avoided in early experiments by using polished electrodes and pressures below atmospheric pressure. This leads to the conclusion that for a fixed surface charge density and an approaching electrode, breakdown will occur at gaps larger than about 10 μm.

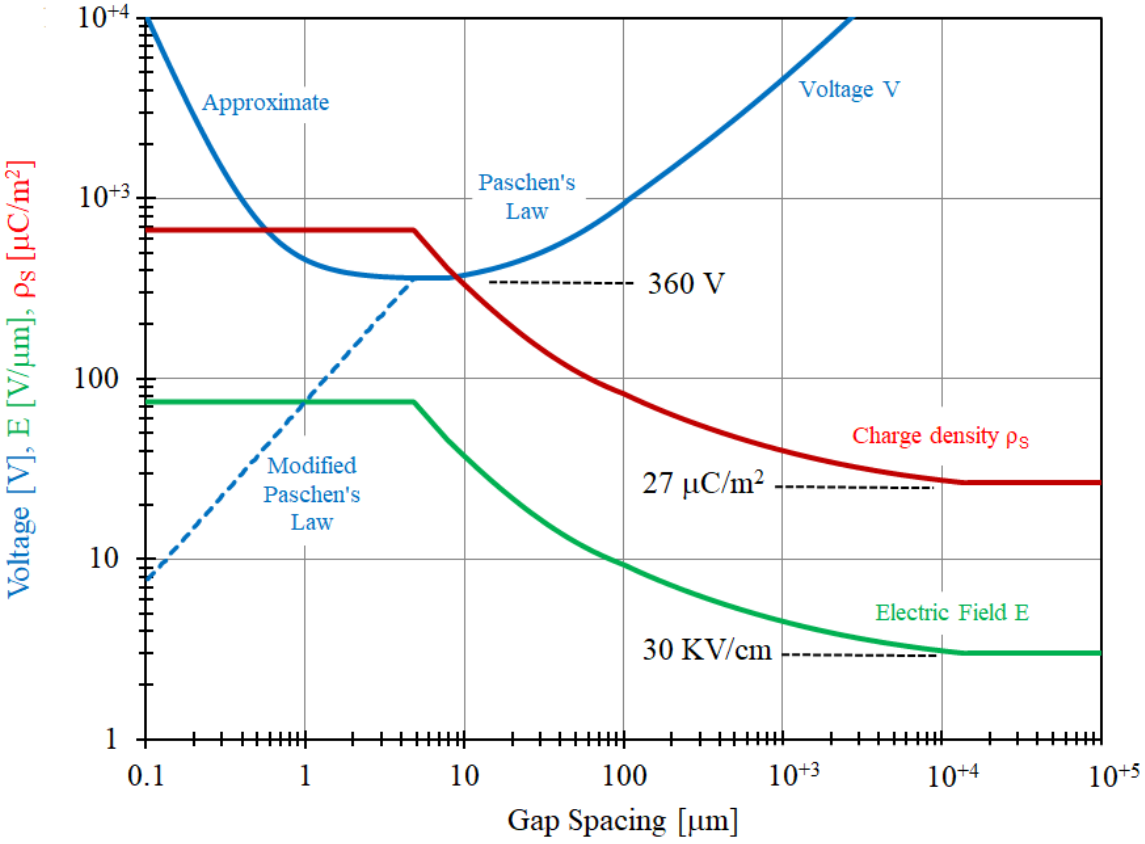

Figure 4. The Paschen curve (1 At pressure) and implications for electrostatic field and charge density required for breakdown.

The following 6-part expression summarizes experimentally observed breakdown voltages (see Annex).

$$V_{Paschen}(d)=\begin{cases} 360(V)+100\times\left\{\left[\frac{1(\mu m)}{d(\mu m)}\right]^2-\left[\frac{1(\mu m)}{4.8(\mu m)}\right]^2\right\} & ; \quad 0.01\le d<4.8(\mu m)\ (\text{Approximate}) \\ 75\left(\frac{V}{\mu m}\right)\times d(\mu m) & ; \quad 0.01\le d<4.8(\mu m)\ (\text{Modified Curve}) \\ 360(V) & ; \quad 4.8\le d<\frac{48}{6.2}(\mu m) \\ 360(V)+6.2\left(\frac{V}{\mu m}\right)\times\left[d(\mu m)-\frac{48}{6.2}(\mu m)\right] & ; \quad \frac{48}{6.2}\le d<100(\mu m) \\ 2.44\left(\frac{V}{\mu m}\right)\times d(\mu m)+65.3\left(\frac{V}{\sqrt{\mu m}}\right)\sqrt{d(\mu m)}+\frac{3500(\mu mV)}{d(\mu m)} & ; \quad 100\le d<13598(\mu m) \\ 3\left(\frac{V}{\mu m}\right)d(\mu m) & ; \quad 13598(\mu m)\le d \end{cases}$$

The electric field E in Figure 4 is the Paschen breakdown voltage $V_{Paschen}$ divided by the gap d, which is the uniform electric field across the gap.

$$E_{Paschen} = \frac{V_{Paschen}}{d}$$

The charge density ρ_s in Figure 4 is the uniform charge density on each side of the gap determined by the electric field E.

$$\rho_s = \varepsilon_0 E_{Paschen}$$

Britton [13] gave equations based on Heidelberg [14] allowing calculation of the axial electrostatic field E_z as a function of distance z from the charged sheet.

$$E_z(z) = -\frac{\sigma_{Sheet}}{2\varepsilon_0}\left\{1 - \frac{D+R-z}{\sqrt{(D+R-z)^2 + \left(\frac{L_{Sheet}}{2}\right)^2}} - \frac{R(D+R)}{z^2} + \frac{2R^3}{z^3} - \frac{R}{z^2}\frac{\left(D+R-\frac{R^2}{z}\right)\left(\frac{2R^2}{z}-D-R\right) - \left(\frac{L_{Sheet}}{2}\right)^2}{\sqrt{\left(D+R-\frac{R^2}{z}\right)^2 + \left(\frac{L_{Sheet}}{2}\right)^2}}\right\}$$

Evaluate this expression for z=D to find the electric field at the tip of the spherical electrode having radius R as a function of gap D from the plane to the tip of the spherical electrode. L is the circular disc diameter having charge density σ_{sheet}.

$$E_z(D) = -\frac{\sigma_{Sheet}}{2\varepsilon_0}\left\{2 - \frac{D}{R} - \frac{2 - \frac{D}{R} - \frac{L^2}{4RD}}{\sqrt{1 + \frac{L^2}{4D^2}}}\right\}$$

This confirms that the axial field on the electrode tip at z = D decreases with increasing gap D and electrode diameter R (Figure 5).

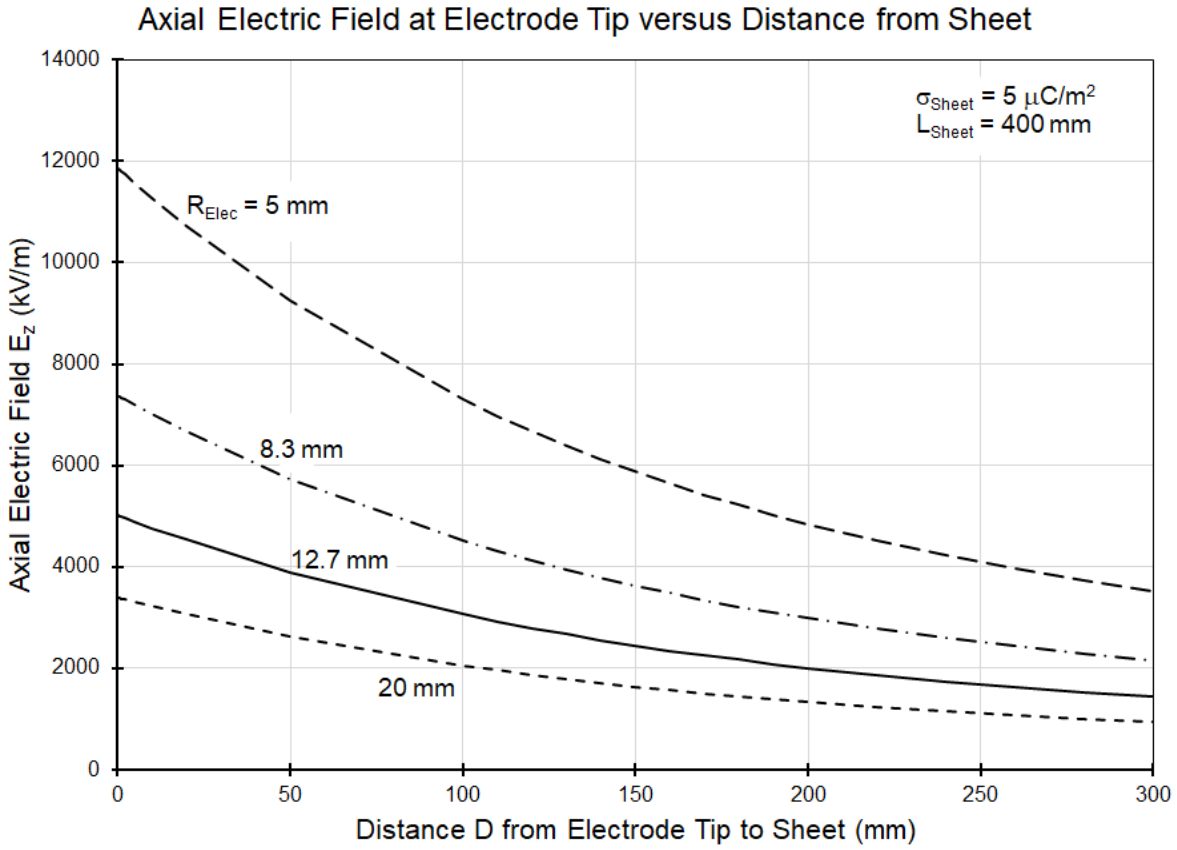

Figure 5. Field at electrode tip for 5, 8.3, 12.7 and 20 mm sphere radius (10, 16.3, 25.4 and 40 mm diameter) and 400 mm diameter target at 5 µC m^{-2} charge density

Breakdown between a charged 400 mm diameter target and our electrodes is suppressed when the electric field is less than the Paschen field. The critical charge density σ_{Crit} makes the axial electric field equal to the Paschen field (Figure 6).

$$\sigma_{Crit}(D) = \frac{2\varepsilon_0 E_{Paschen}(D)}{\left(2 - \frac{D}{R} - \frac{2 - \frac{D}{R} - \frac{L^2}{4RD}}{\sqrt{1 + \frac{L^2}{4D^2}}}\right)}$$

$$E_{Paschen} = \frac{V_{Paschen}}{d} = \begin{cases} 75\left[\frac{V}{\mu m}\right] & ; \quad 0 \le d \le 4.8\ \mu m \\ \frac{360\ [V]}{d\,[\mu m]} & ; \quad 4.8 \le d \le \frac{48}{6.2}\ \mu m \\ \frac{360[V]}{d\,[\mu m]} + 6.2\left[\frac{V}{\mu m}\right]\left(1 - \frac{\frac{48}{6.2}[\mu m]}{d\,[\mu m]}\right) & ; \quad \frac{48}{6.2} \le d \le 100\ \mu m \\ 2.44\left[\frac{V}{\mu m}\right] + 65.3\left[\frac{V}{\sqrt{\mu m}}\right]\frac{1}{\sqrt{d\,[\mu m]}} & ; \quad 100 \le d \le \sim 1000\ \mu m \\ 3\left[\frac{V}{\mu m}\right] & ; \quad \sim 1000\,\mu m \le d \end{cases}$$

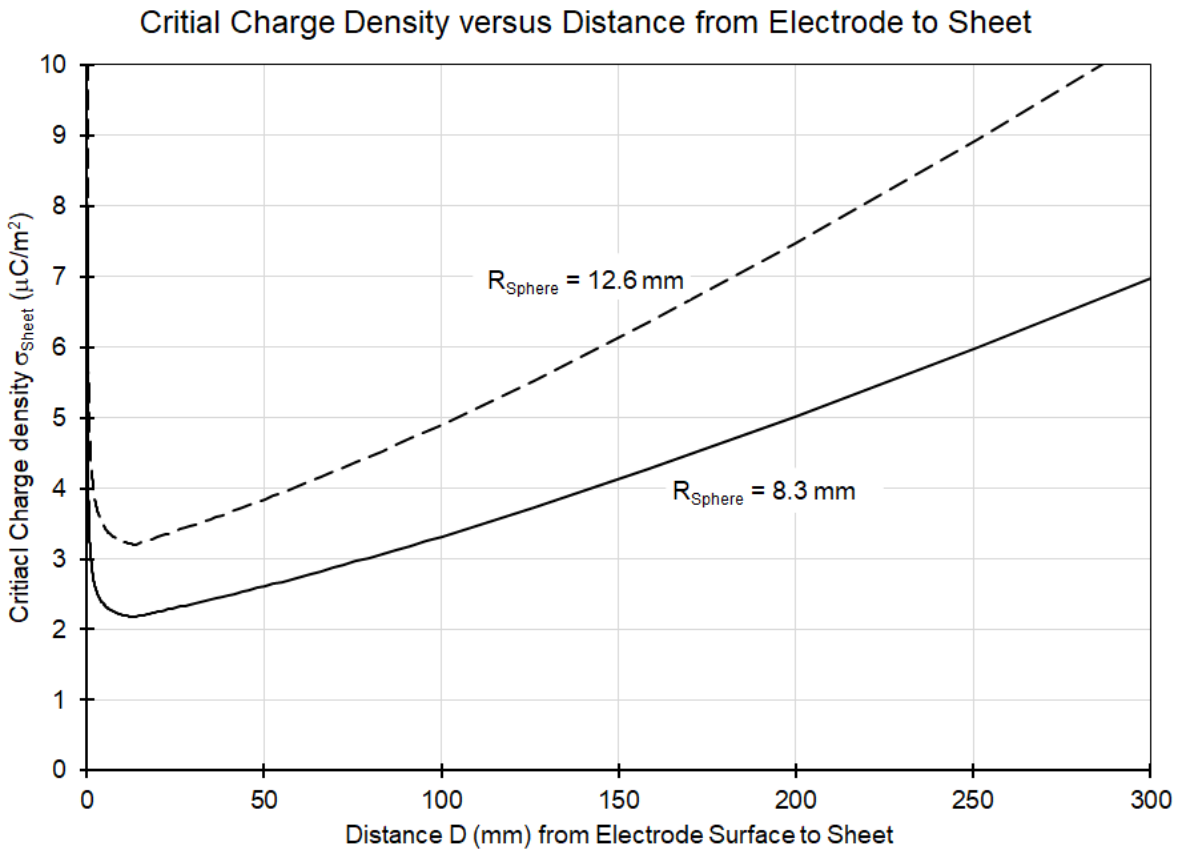

Figure 6. Critical target charge density for the onset of ionization at the tip of 12.6 and 8.3 mm radius (16.6 and 25.4 mm diameter) electrode

The axial electric field at the electrode tip is the maximum electric field when the electrode is far from the charged, circular disc. When the gap between the electrode tip and the charged, circular disc is less than about 1 cm, the critical charge density increases sharply because the Paschen electric field increases (see Figure 2). At small gaps *D*, the maximum electric field also shifts away from the electrode tip [17]. The increase in the Paschen field at small gaps together with the shift in the maximum electric field away from the tip suggest that discharges will occur away from the electrode tip.

In this work, we focus on discharges that occur at gaps *D* larger than 1 cm when the charge densities exceed the minimum.

4 Computer modelling

The electrical field, potential and charge were investigated by numerical simulation in the commercial software COMSOL, which uses Finite Element Analysis. This was used to solve Maxwell's equations in the electrostatic approximation for an irrotational electric field by discretising problem spaces into a mesh of "elements" defined by nodes and edges. The solution inside each element is defined by an approximate polynomial function, and the full problem space calculation is reduced to only solving for the values at the nodes. Electrostatic solutions are generally used where dielectrics can be considered to be ideal and all materials have a permittivity and zero conductivity. Conductors are typically represented by boundaries of equal electrical potential. The electric field and charges in the system are determined by solving Poisson's equation for the electric field **E**:

$$\nabla \cdot (\varepsilon \mathbf{E}) = \rho \qquad \text{or} \qquad \nabla \cdot (\varepsilon \nabla \phi) = -\rho$$

where ϕ is the electric field, ε is the electrical permittivity of the material(s) and ρ is the free charge density.

The experimental arrangement was modelled as a simple axisymmetric sphere-plane geometry, cylindrically symmetrical around the mutual central axis of the electrode and the holder. This required simplification of the square target a 200 mm radius plane, defined as a surface having fixed charge density of 5 μCm^{-2}.

The problem space for the simulations is shown in Figure 7a), with the charged target plate, the measurement electrode and the holder defined as boundaries around a homogeneous material. All charges are assumed to be bound rather than free and with a homogeneous material, the solution of the electrical potential and the electric field is dependent only on the geometry of the system and not on the properties of the material. The general equation then reduces to Laplace's equation:

$$\nabla^2 \phi = 0$$

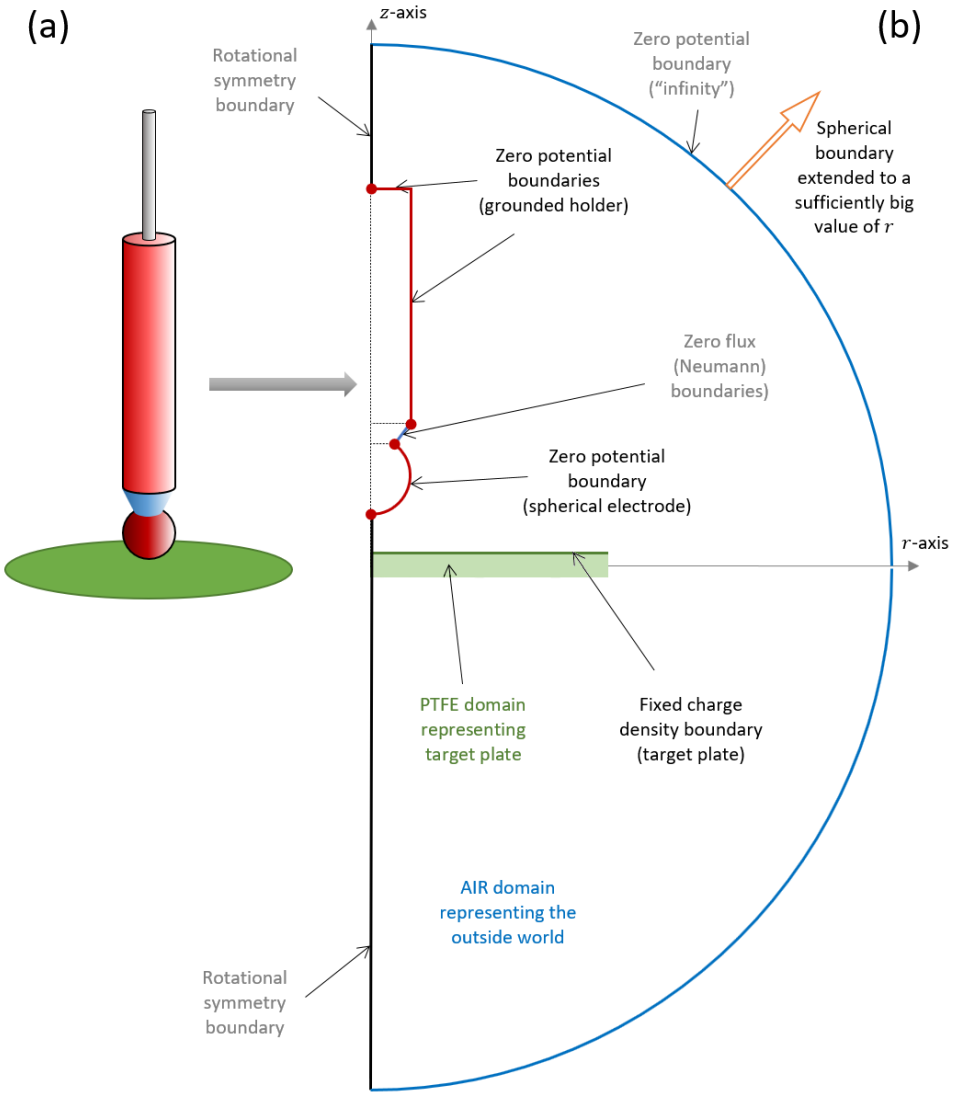

Figure 7. Computer model of probe and charge insulating plane

The boundary conditions for the rotationally symmetrical problem space are shown in Figure 7b. The spherical electrode and the holder were defined as metallic zero potential surfaces. An "infinite" zero potential boundary is defined by the outer quarter circle, which is placed at a distance significantly larger than the target. All other boundaries are zero flux or Neumann boundaries.

5 Results of computer modelling

Figure 8 shows electrostatic field modelling results. Figure 8a shows the field from the target alone in the absence of a measurement electrode. Figure 8b shows the effect of introducing a 25.4 mm diameter charge transfer measurement electrode of the design of Figure 3. The field from the target can clearly be seen to be coupling not just to the spherical measurement electrode tip, but also to the earthed metal handle. In Figure 8c the field coupling to the spherical electrode alone is shown. It can be clearly seen that this coupling is to a limited area of the target, rather than the whole target area.

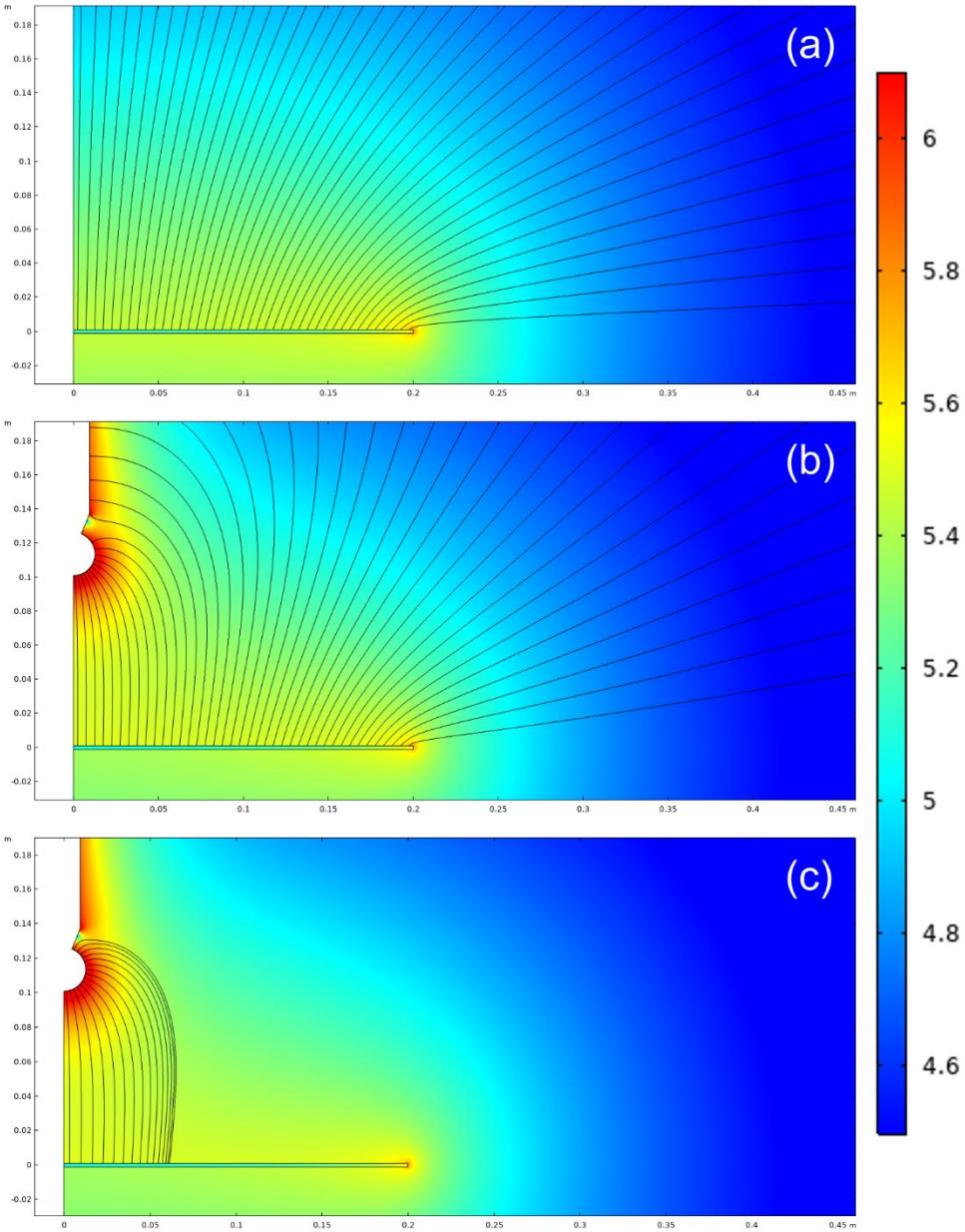

Figure 8. Electrostatic field model results a) field from target with no measurement electrode present b) field with electrode present (gap 100 mm), including handle c) showing the field coupling of the spherical electrode with the target

Figure 9 to Figure 12 show the field strengths found at the target center and electrode tip, as the gap is increased between 1 mm and 1000 mm (log scale).

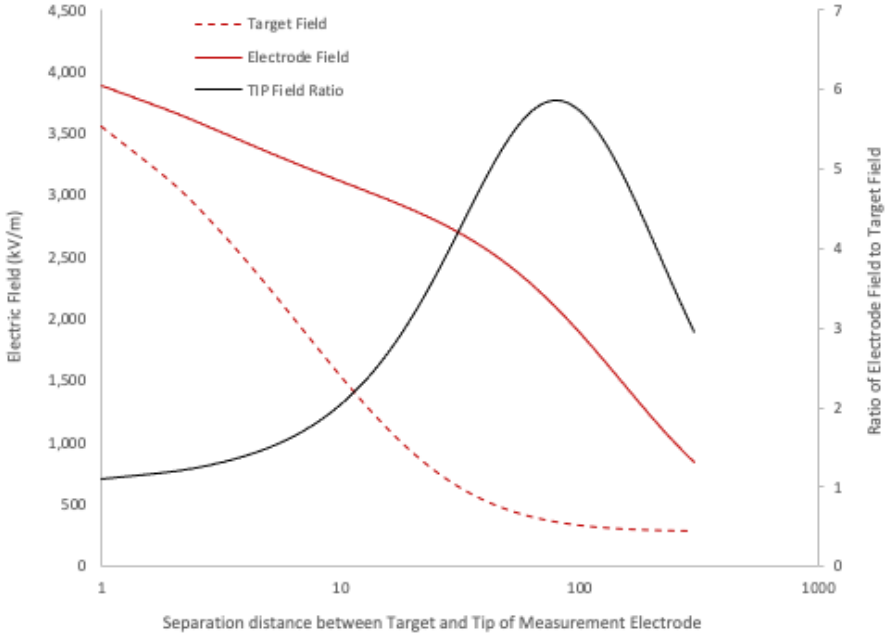

Figure 9. Field at target and electrode tip, and the field ratio (intensification) vs gap in mm - 40 mm sphere

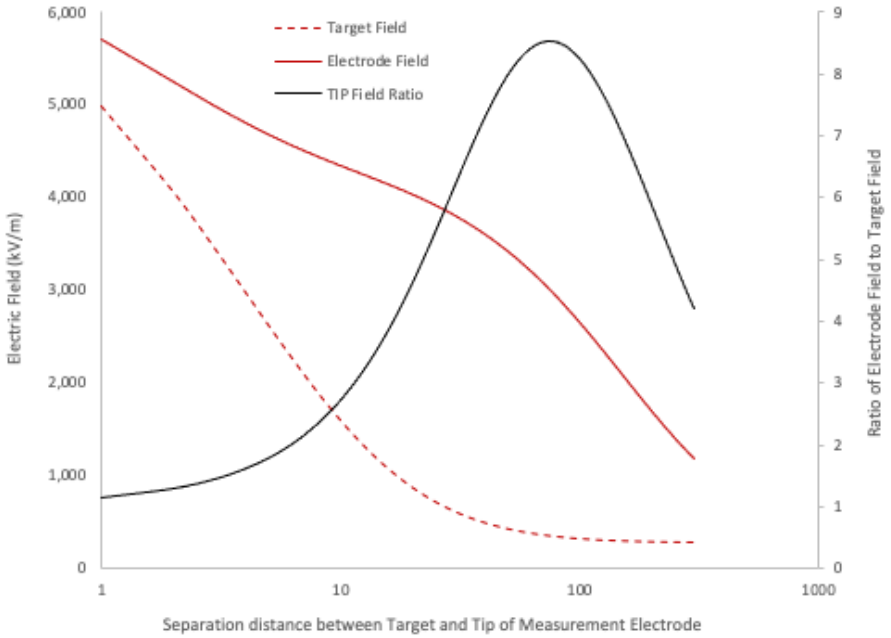

Figure 10. Field at target and electrode tip, and the field ratio (intensification) vs gap in mm - 25 mm sphere

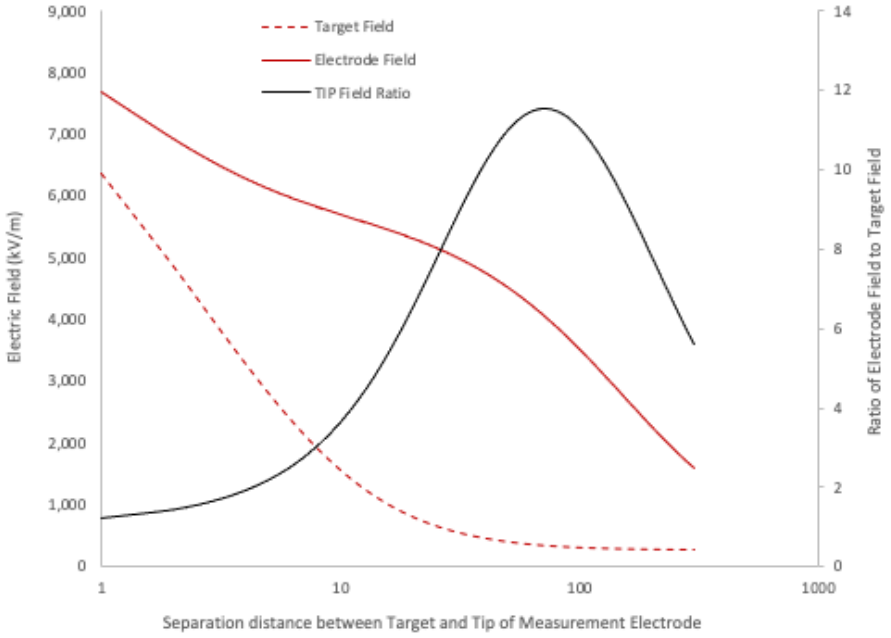

Figure 11. Field at target and electrode tip, and the field ratio (intensification) vs gap in mm - 16.6 mm sphere

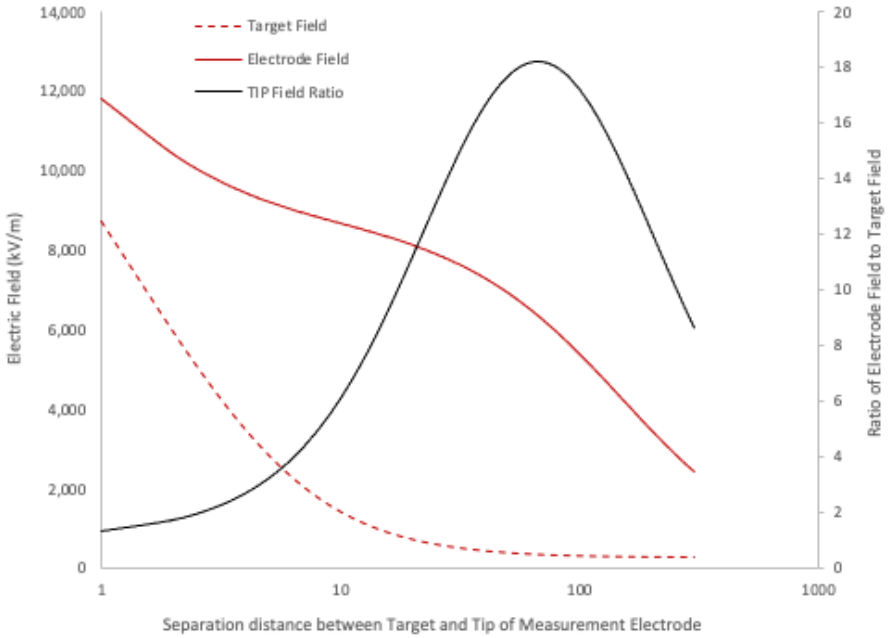

Figure 12. Field at target and electrode tip, and the field ratio (intensification) vs gap in mm - 10 mm sphere

6 Experimental results

6.1 Charge density calibration

An EFM51 electrostatic field meter was fitted with a 194 x 161 mm earthed field plate made from copper clad epoxy material. The field reading from this showed good agreement with the calculated field from a metal plate at 100 V at known distance from the meter.

The surface charge density calculated from field meter readings for various corona charging voltages (average of 3 runs) is shown in Figure 13. The results show reasonable reproducibility although there is some indication of "flattening off" above 12 kV.

In contrast, the induced charge Q_i on 16.6 mm and 25.4 mm probes held at 20mm from the target show a linear rise with corona voltage up to 13 kV. Discharges were observed at 13 kV corona voltage for the 25 mm probe and 11 kV for the 16 mm probe in this arrangement, corresponding with 54 nC and 26 nC induced charge respectively.

This figure suggests that the field meter measurements show variation from an unknown source at higher field strengths. This variation is not shown in the induced charge on the spherical probes, suggesting that it is linked to use of the field meter. The meter has an annular projection around the sensor window. This might go into corona discharge at high electrostatic field and reduce the charge density on the target. The charge density indicated by probes induced charge showed better linearity than indicated by meter readings. Neither probe showed any flattening off of the response at the corona voltage levels tried.

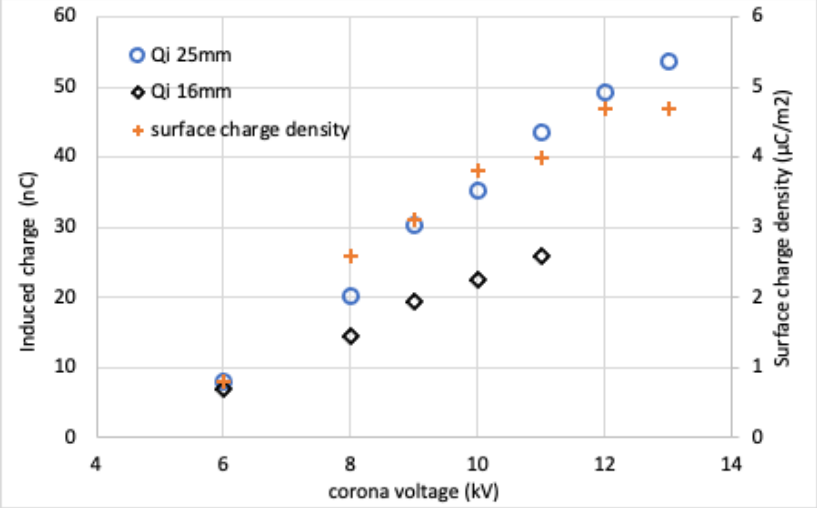

Figure 13. Induced charge on 16.6 mm and 25.4 mm probes at 20 mm distance, and charge density calculated from electrostatic field readings, vs corona voltage.

Both the field meter and induced charge measurement results are likely to depend on the effect of charge density over a significant area of the target surface rather than small area local charge density. Although no attempt was made to verify the small area local charge density variation, the results are consistent with reasonably reproducible and constant charge density over the surface.

6.2 Variation of field with distance from charged PTFE target measured with and without field plate

The field measured with and without the field linearising plate is shown in Figure 14 as a function of distance from the charged PTFE target. The charging corona voltage was 6 kV. With the field plate fitted, the field was remarkably constant over the range 10 – 50 mm, as predicted by a simple capacitor model [4], [5]. Some reduction was apparent as distance increased above 20 mm and reduced below 10mm.

The indicated field strength of the meter alone E_m was approximately twice the field E with field plate fitted, for distances from 50 mm to 25 mm. As the distance reduced below 25 mm, the ratio E_m/E increased as distance reduced, exceeding 3 at 5 mm distance. It is likely this relationship would vary with the design of the field meter.

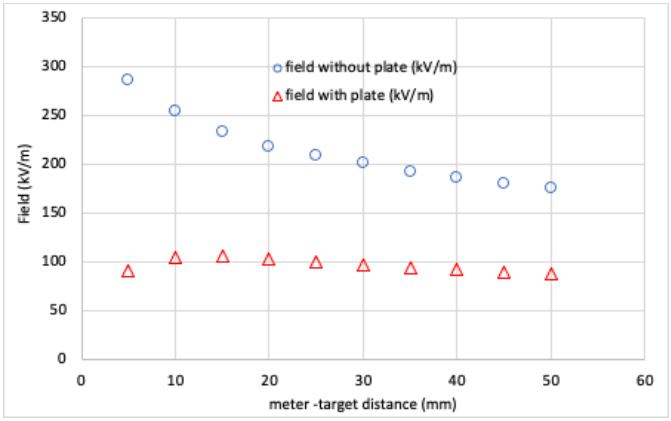

Figure 14. Field measured as a function of distance with and without the field plate

6.3 Induced voltage on probes as a function of distance

The induced charge on the probes as a function of distance is shown in Figure 15.

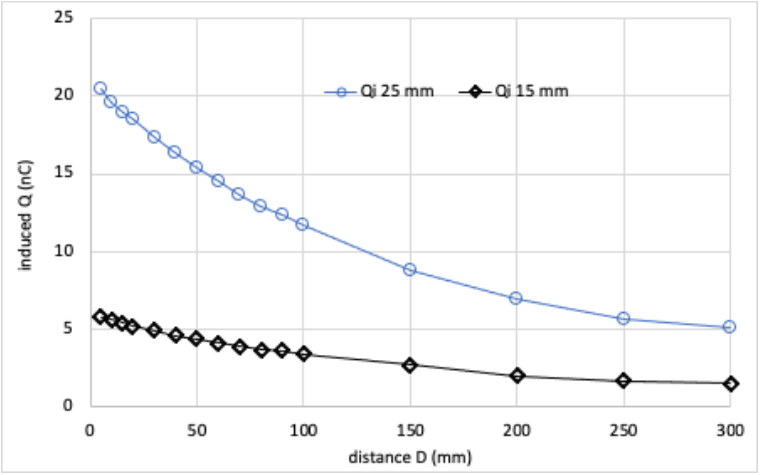

Figure 15. Induced charge on spherical electrodes as function of distance 0 – 300 mm (Vc = 6kV)

It is worth noting that the induced charge remains relatively constant over a small range of distance, especially for the smaller probe. This could make induced charge on a spherical probe a practical means of evaluating the state of charge of a large charged planar insulating surface in industrial processes. Field meters of course operate by induced charge on the sensor plates [14]. Nevertheless, the relation between a field meter reading and the surface charge density is not always clear as it is affected by the meter design and geometry as well as other factors. The spherical probe gives a defined geometry that can clarify this. Against this, used in this way the measurement would be subject to possible errors from coulombmeter drift or corona ion current that could affect results.

6.4 Charge induced and transferred in discharges

The 16.6 mm and 25.4 mm probes were set to just touch the raised target when it was raised.

After charging, the target was raised to position. Typically, after touching and fixing in position the target relaxed to about 1 mm distance from the probe. The total induced and transferred charge was noted in the raised position in Figure 16 for the 16.6 mm probe and in Figure 17 for the 25.4 mm probe. The target was then lowered, and the final accumulated charge measured. Where the transferred charge Q_t was zero, it was presumed that no significant discharge had taken place. This is consistent with the field remaining below a threshold for breakdown of the electrode-target gap but is discussed further in Section 7.2.

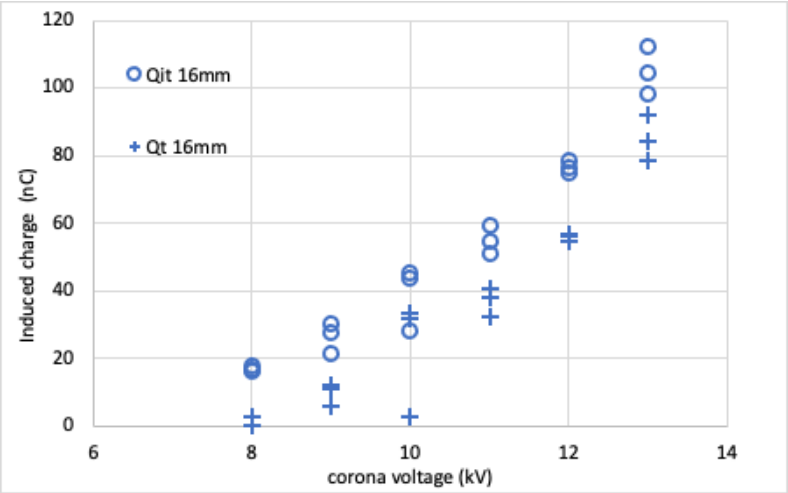

Figure 16. Total induced and transferred charge Q_{it} and transferred charge Q_t vs corona voltage for 16.6 mm probe

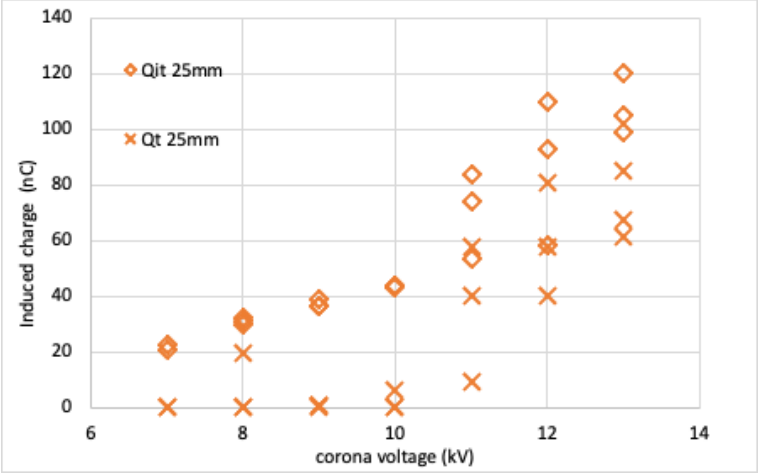

Figure 17. Total induced and transferred charge Q_{it} and transferred charge Q_t vs corona voltage for 25.4 mm probe

The smaller 16.6 mm probe experienced brush discharges at a lower charge density (corona voltage) than the 25 mm probe. Except for one anomalous result at 8kV the 25.4 mm probe did not record discharges below 10 kV corona voltage. The 16.6 mm probe recorded discharges from about 8 kV upwards. This might be consistent with higher field strengths at the surface of the smaller probe.

Nevertheless, when discharges ensued with the 25.4 mm probe they tended to have higher charge transferred in the discharge.

This was investigated further by moving electrodes in from a distance (500 mm) by hand along the concentric axis of the target.

The induced and transferred charge in discharges was recorded using computer based oscilloscope software. The recording was started and the electrode then moved by hand along the axis towards the target by sliding the retort stand along the guide and rule. The rate of approach was estimated to be around 20 mm s^{-1}. This simulates the situation in which a hand held probe is brought towards a target during a practical charge transfer test such as described in [2].

As the electrode approached the charged target until either a discharge occur or the target was touched. The electrode approach was halted at this point and the charge and distance at which this occurred noted from the rule. The electrode was then be withdrawn to 500 mm distance and the final charge accumulated by the coulombmeter could then be measured. A typical waveform is shown in Figure 18.

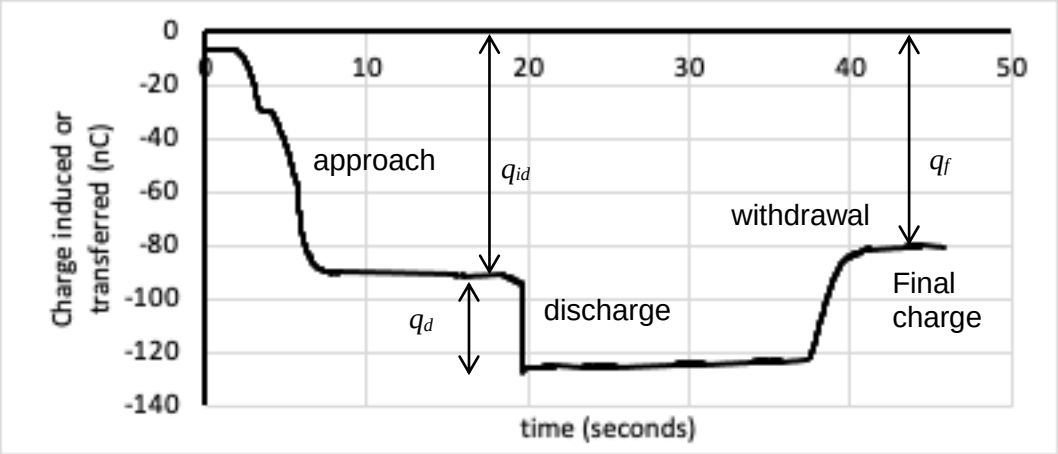

Figure 18. Charge induced and discharged to 25 mm electrode as electrode was moved from 500 mm distance to discharge point and then returned to 500 mm distance (V= – 20 kV)

The charge induced threshold at the time of discharge q_{id}, and the charge transferred in the discharge q_d, and the final charge q_f accumulated by the coulombmeter could be measured from the waveform. In the example waveform above, the values are 95 nC, 33 nC and 80 nC respectively, with the discharge occurring at 4 mm gap. Waveforms without discharges lacked the fast step corresponding to charge being transferred.

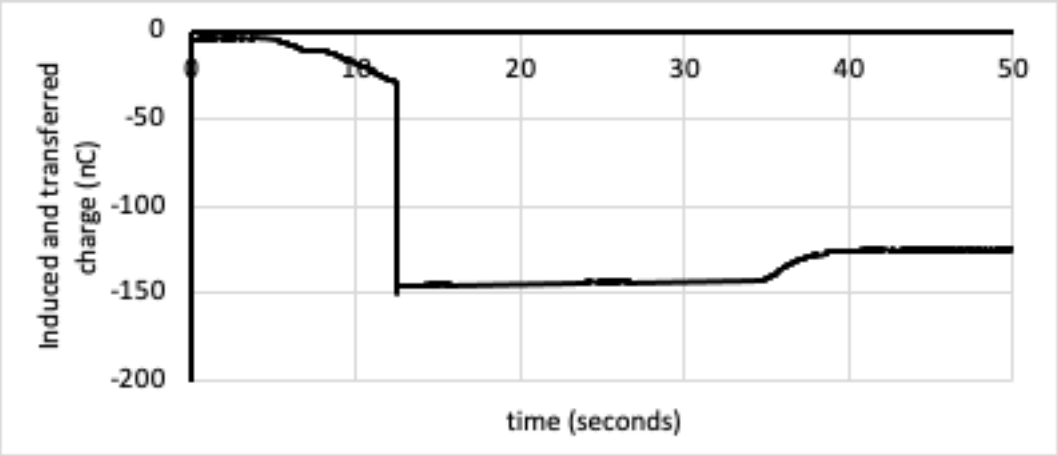

Figure 19 Charge induced and discharged to 16.6 mm electrode as the electrode was moved from 500 mm distance to discharge point and then returned to 500 mm distance (V= – 20 kV)

Figure 19 shows a similar waveform obtained with the 16.6 mm diameter electrode. In this case the values obtained for q_{id}, q_d, and q_f were 29 nC, 121 nC and 125 nC respectively, with the discharge occurring at 60 mm gap.

The values obtained for q_{id}, q_d, and q_f were recorded, with the gap at which discharge occurred, for several discharges with both electrodes at various corona charging voltages (Table 1). There was considerable variation in discharges obtained in this way, and the resulting values.

Table 1. Induced charge threshold of discharge the charge transferred in the discharge q_d, and the final charge q_f accumulated by the coulombmeter in recorded discharges

Electrode dia (mm)	Corona voltage (kV)	Threshold of discharge q_{id} (nC)	Transferred charge q_d (nC)	Final charge q_f (nC)	ESD detected	Discharge gap (mm)
25.4	18	73	33	66	Yes	12
25.4	20	95	33	80	Yes	12
25.4	20	73	97	132	Yes	32
25.4	20	92	39	92	Yes	8
16.6	20	29	121	125	Yes	60
16.6	20	109	30	115	Yes	60
16.6	20	84	28	90	Yes	65
16.6	16	28	47	55	Yes	38
16.6	16	29	65	74	Yes	23
16.6	12	n/a	0	< 1	No	touched
16.6	14	28	25	39	Yes	1
16.6	15	27	30	39	Yes	9
16.6	15	28	34	44	Yes	6
16.6	15	27	26	34	Yes	6

7 Discussion

7.1 Measurement of field and surface charge density

The field meter reading when not fitted with the field linearizing plate was about twice the field strength confirmed with the plate fitted at a distance of 25 mm (Figure 9). As the instrument is supplied for use without a linearising plate it suggests that in normal use with gap around 25 mm the field measured in a practical situation would be overestimated approximately by a factor of 2. This overestimation at least would be expected to give an additional factor of safety if the field meter is used for surface charge measurement in hazard evaluation. This does not consider any influence of an earthed operators hand holding the instrument or their body nearby, which would be expected to reduce the reading and reduce any safety factor.

7.2 Charge transferred in the discharge

The charge transferred for both probes is compared in Figure 20 with 10 nC and 60 nC levels. The significance of these is that in hazard evaluation, 10 nC is given as the maximum acceptable limit for Group IIC materials in Zone 1 or Zone 2. The 60 nC limit is given for Group IIA materials (Table 4 in [2]).

There is a suggestion here that when used in charge transfer measurements for hazard evaluation with surface charge levels near the threshold of discharge, a 16.6 mm electrode would show risk for Group IIC materials at lower surface charge density (corona voltage) than a 25.4 mm probe. This raises the question whether smaller probes might continue this trend.

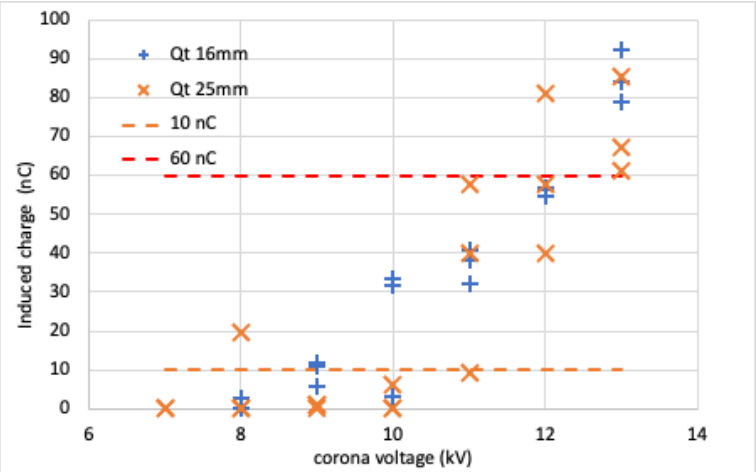

Figure 20. Charge transferred compared for both probes with 10 nC and 60 nC lines

The lack of measured charge transfer observed in Section 6.4 was stated to be consistent with consistent with a lack of ESD occurring. Nevertheless, there is another possibility that should be discussed. At the same time it is interesting to note that when a discharge occurs, the combined induced and transferred charge is typically much higher than was expected for induced charge alone.

It has long been recognized that in charge transfer measurements not all the charge available to ESD is measured in the discharge circuit [18]. This is because the field from a fraction of the charge couples to the discharge probe, but the remainder couples to nearby earthy conductors or other objects. This is clearly seen in or model field plots of Figure 8 b and c. Before ESD occurs, the portion of the charge coupling to the probe (Figure 8c) is recorded as the equal and opposite polarity charge is induced on the electrode. On ESD occurring, however, this charge is merely neutralized by the discharge between the electrode and the target surface. The fraction of charge in the discharge that is recorded is presumably that which originates outside the area that couples to the electrode, and couples to the shield and other nearby conductors. This is consistent with charge transferred in the ESD being not obviously related to than the induced charge and perhaps indicates that the otherwise unmeasured part of the charge could be found from the induced charge on the electrode.

So, a possible alternative explanation for lack of measured charge transfer occurring on the electrode touching the target, or at small gaps near the threshold conditions for ESD to occur, is that the charge transferred originates from the patch that is coupled to the electrode alone. This might, however, be expected to show as results in which the transferred charge appears zero but a final charge (Figure 18) is non-zero. In our limited experiments this has so far not been observed.

7.3 Induced charge threshold for onset of discharge

The induced charge in the probe appears related to the target charge density level at which discharges commence. In experiments with the probes set at 20 mm from the target (Figure 13), discharges commenced at 13 kV for the 25.4 mm probe and 11 kV for the 16.6 mm probe. Calculating the surface area of each and combining at a maximum charge density for breakdown of 26 µC m^{-2}, gave predicted onset of discharges at 54 nC and 26 nC respectively. These approximate the induced charges levels at which discharges were sometimes observed. Various workers [8], [9], [10] have commented that the surface field required for breakdown at the surface of a spherical electrode increases as the electrode diameter is reduced. So, in practice the threshold for discharges occurring is likely to be higher than these values. It also seems from our approaching electrode results that a discharge does not necessarily occur as soon as the field strength is sufficient. There may be unidentified probabilistic and other factors which influence the onset of a discharge. This would explain why the induced charge threshold is often much greater than the anticipated breakdown level before discharges occur, and there is considerable variation in discharge gap for otherwise apparently similar conditions. Indeed, a discharge did not always occur when conditions appeared to be sufficient. The field criteria may indicate one of several factors that are required to initiate a discharge. Further work is required to understand these issues.

8 Conclusions

This work has focused on some areas around the conditions surrounding the evaluation of electrostatic discharge risks in hazard evaluation where an object (field meter or discharge electrode) approaches a charged insulating surface. Many of these were already known issues, but this work has aimed to clarify, understand and quantify them to some extent using analytic, computer modelling and experimental techniques.

While it is known that a field meter without field linearizing plate will "see" an increase the measured field, this is how they are most often used in practice. We have quantified this for our EFM51 instrument. This was found to approximately double the field measured from a charged surface when held around 25 mm from the surface. Other instruments and operating conditions are likely to give different results. Direct comparison suggests that in some cases the charge induced on a spherical electrode could be usefully used to evaluate the surface charge density of an insulator providing the characteristics of the probe are known.

The field at the surface of the charged insulator target remains approximately constant for gaps greater than about 100 mm as the electrode approaches the target. Conversely, the field at the electrode tip increases strongly as gap is reduced below around 500 mm. A peak is shown in intensification for a gap just less than 100 mm although the field at the probe surface continues to increase as the gap is reduced. The field intensification at the electrode increases with reducing electrode diameter and was around 12 for a 16.6 mm and 8.5 for a 25 mm sphere. This confirms that a considerable safety factor should be taken into account in cases where small earthed objects might approach a charged surface and target surface charge density is used to evaluate ESD risk.

For a spherical electrode, one condition for the onset of discharge from the electrode corresponds to the charge on the sphere surface that gives a breakdown surface charge density and field strength. This charge density is dependent on the diameter of the electrode. A smaller electrode requires a smaller induced charge for discharge. Below the threshold of discharge, no significant charge was transferred even when the electrode touched the charged surface. Achievement of the critical electrode surface charge density did not always result in a discharge, which suggests that other factors might also be influential. Considerable variation was found in threshold of discharge, discharge gap and charge transferred in discharges obtained in apparently similar conditions.

Our analysis suggests that discharges could occur at electrode-target gaps around 10-20 mm at lower target surface charge density than with gaps below 10 mm. This supports the view that at smaller gaps discharges could preferentially occur from the side of the electrode rather than at the axis closest point. In practical experiments, onset of discharge occurred at a lower target surface charge density for the smaller 16.6 mm diameter spherical electrode, when surface charge density was near the threshold for discharge occurring. This suggests that evaluation of discharge risk to sensitive Group IIC gases by charge transfer in discharges from a charged surface might be better done with smaller electrodes than currently specified by the standards.

Conversely, above the threshold where discharges occur, higher charge transfer was obtained with the 25.4 mm diameter electrode. This diameter electrode is suited for evaluating the risk of ignition to Group IIA gases by charge transfer in discharges from a charged surface.

Given the variability of discharges and small number of our experiments, these findings would benefit from further work for confirmation.

Funding: This work did not receive any specific grant from funding agencies in the public, commercial, or not-for-profit sectors.

ANNEX 1: Paschen's Law

The breakdown voltage between two surfaces varies with the product of gas number density *n* and the gap *d* between the surfaces. This variation in breakdown voltage with (*nd*) is known as Paschen's law [12]. The following six expressions extend work on the Paschen curve by Mark Zaretsky (M. Zaretsky, personal communication, 5/19/1999).

For large gaps greater than about 1.4 cm, the breakdown voltage in (1) has a slope of 3 V/μm, which is the breakdown strength of air at atmospheric pressure.

$$V_{Paschen}(d) = 3\left(\frac{V}{\mu m}\right) d(\mu m) \quad ; \quad 13598(\mu m) \le d \tag{1}$$

For gap less than 1.4 cm down to 100 μm, the breakdown voltage (2) has been investigated extensively [12].

$$V_{Paschen}(d) = 2.44\left(\frac{V}{\mu m}\right) \times d(\mu m) + 65.3\left(\frac{V}{\sqrt{\mu m}}\right)\sqrt{d(\mu m)} + \frac{3500(\mu m V)}{d(\mu m)} \quad ; \quad 100 \le d < 13598(\mu m) \tag{2}$$

The breakdown voltages for large gaps down to 100 μm are most relevant to discharges between small radius objects and charged planar insulating materials.

For gaps less than 100 μm down to the Paschen minimum (~7.5 μm), the breakdown voltage in (3) varies linearly with gap *d*. This linear segment simply connects the well-established result (2) with the Paschen minimum breakdown voltage.

$$V_{Paschen}(d) = 360(V) + 6.2\left(\frac{V}{\mu m}\right) \times \left[d(\mu m) - \frac{48}{6.2}(\mu m) \right] \quad ; \quad \frac{48}{6.2} \le d < 100(\mu m) \tag{3}$$

Near the Paschen minimum (~7.5 μm), the minimum breakdown voltage in air at atmospheric pressure in well-controlled laboratory experiments is 327 V [16]. In practical applications including, for example, electrophotographic electrostatic transfer, the Paschen minimum breakdown voltage in (4) is found to be about 360 V [11].

$$V_{Paschen}(d) = 360(V) \quad ; \quad 4.8 \le d < \frac{48}{6.2}(\mu m) \tag{4}$$

For gaps less than 4.8 μm (small gaps), the voltage in (5) has a slope of $7.5\times10^{+5}$ V/cm or 75 V/μm [12] that is limited by non-linear effects such as field emission. This limited voltage is not a breakdown voltage because gas-phase ionization does not determine the current. This voltage limit is a modification to the Paschen curve.

$$V_{Paschen}(d) = 75\left(\frac{V}{\mu m}\right) \times d(\mu m) \quad ; \quad 0.01 \le d < 4.8(\mu m) \tag{5}$$

For gaps less than 4.8 mm (small gaps), the Paschen breakdown voltage increases with decreasing gap. This increase in breakdown voltage is observed primarily at pressures well below atmospheric pressure. The approximate, empirical expression (6) illustrates this behavior with the breakdown voltage varying as d^{-2}.

$$V_{Paschen}(d) = 360(V) + 100 \times \left\{ \left[\frac{1(\mu m)}{d(\mu m)} \right]^2 - \left[\frac{1(\mu m)}{4.8(\mu m)} \right]^2 \right\} \quad ; \quad 0.01 \le d < 4.8(\mu m) \tag{6}$$

References

[1] N. Gibson, Lloyd FC, Incendivity of discharges from electrostatically charged plastics. Brit. J App. Phys Vol 16 (1965)

[2] International Electrotechnical Commission, Explosive atmospheres Part 32-1. Electrostatic hazards, guidance, IEC TS 60079-32-1:2013 + A1:2017

[3] International Organisation for Standardisation (ISO), Explosive atmospheres. Part 36: Non-electrical equipment for explosive atmospheres – Basic method and requirements. ISO 80079-36:2016

[4] A. E. Seaver, Analysis of electrostatic measurements on non-conducting webs, J. Electrostatics 35 (1995), 231-243.

[5] K. Robinson, J. Smallwood, Electrostatic risk and specification of field and voltage limits for insulating web materials. (2019) Phys. Conf. Ser. 1322 012021

[6] International Electrotechnical Commission. Explosive atmospheres Part 32-2. Electrostatic hazards - Tests. IEC 60079-32-2:2015

[7] CEN, Non-electrical equipment for use in potentially explosive atmospheres – Part 1: Basic method and requirements, EN13463-1:2009

[8] N. J. Felici, Electrostatics and electrostatic engineering. Proc. Static Electrification Conference. (1967)

[9] K. G. Lövstrand, The ignition power of brush discharges—experimental work on the critical charge density. Journal of Electrostatics 10 (1981) 161-168.

[10] L. Dascalescu, P. Ribardière, C. Duvanaud, J. M. Paillot, Electrostatic discharges from charged spheres approaching a grounded surface. J. Electrostatics (1999) 47.4 249-259.

[11] R. M. Schaffert, Electrophotography 2nd ed., Focal Press Limited, London, (1975) ISBN 0803819412, pg 514-519.

[12] R. M. Meek, J. D. Craggs, Electrical Breakdown in Gases, John Wiley and Sons, Ltd., New York, NY, (1978), ISBN-10: 0471995533.

[13] L. Britton, Avoiding Static Ignition Hazards in Chemical Operations, Center for Chemical Process Safety of the American Institute of Chemical Engineers, New York, (1999) ISBN 0-8169-0800-1.

[14] E. Heidelberg, Generation of Igniting Brush Discharges by Charged Layers on Earthed Conductors, 1967 Static Electrification Conference, Institute of Physics, London.

[15] P. E. Secker, The use of field mill instruments for charge density and voltage measurement. Int. Phys. Conf. Ser. No. 27 (1975) 173-181

[16] *Paschen Curve: Voltage Breakdown vs Pressure*, HighVoltageConnection.com, 2003, www.highvoltageconnection.com/articles/paschen-curve.html, accessed 12/16/2021

[17] Z. J. Grabarczyk, Measurement of electric charge transferred by brush discharge from electrified dielectric or conducting surface – differences and potential source of error, Przegląd Elektrotechniczny, ISSN 0033-2097, R.89 NR 12/2013.

[18] J. N. Chubb, Measurement of charge transfer in electrostatic discharges, J. Electrostatics (2006) 64 pp 321-325

Declaration of interests

☒The authors declare that they have no known competing financial interests or personal relationships that could have appeared to influence the work reported in this paper.

☐The authors declare the following financial interests/personal relationships which may be considered as potential competing interests: